1/5 and 1/3 Magnetization Plateaux in the Spin 1/2 Chain System $YbAlO_3$

P. Mokhtari,[1,2,3,*] S. Galeski,[2,4] U. Stockert,[3] L. Behera,[3] S. E. Nikitin,[5] R. Wawrzyńczak,[2] R. Küchler,[2] M. Brando,[2] L. Vasylechko,[6] O. A. Starykh,[7,†] and E. Hassinger[3,2,‡]

[1]*Department of Physics, Technical University of Munich, 85748 Garching, Germany*
[2]*Max Planck Institute for Chemical Physics of Solids, 01187 Dresden, Germany*
[3]*Technische Universität Dresden, 01062 Dresden, Germany*
[4]*Physikalisches Institut, Universität Bonn, Nussallee 12, 53115 Bonn, Germany*
[5]*Laboratory for Neutron Scattering and Imaging, PSI Center for Neutron and Muon Sciences, Paul Scherrer Institut, CH-5232 Villigen-PSI, Switzerland*
[6]*Lviv Polytechnic National University, Lviv 79013, Ukraine*
[7]*Department of Physics and Astronomy, University of Utah, Salt Lake City, Utah 84112-0830, USA*

(Received 28 December 2024; revised 18 April 2025; accepted 20 May 2025; published 13 August 2025)

Quasi-one-dimensional magnets can host an ordered longitudinal spin-density wave state (LSDW) in magnetic field at low temperature, when longitudinal correlations are strengthened by Ising anisotropies. In the $S = 1/2$ Heisenberg antiferromagnet $YbAlO_3$ this happens via Ising-like interchain interactions. Here, we report the first experimental observation of magnetization plateaux at 1/5 and 1/3 of the saturation value via thermal transport and magnetostriction measurements in $YbAlO_3$. We present a phenomenological theory of the plateau states that describes them as islands of commensurability within an otherwise incommensurate LSDW phase and explains their relative positions within the LSDW phase and their relative extent in a magnetic field. Notably, the plateaux are stabilized by ferromagnetic interchain interactions in $YbAlO_3$ and consistently are absent in other quasi-1D magnets such as $BaCo_2V_2O_8$ with antiferromagnetic interchain interactions. We also report a small, steplike increase of the magnetostriction coefficient, indicating a weak phase transition of unknown origin in the high-field phase just below the saturation.

DOI: 10.1103/grfl-37g2

Introduction—Low-dimensional quantum magnets support a large variety of exotic quantum states, such as quantum spin liquids [1], magnetization plateaux, or nematic states that are induced by quantum fluctuations [2]. Quasi-one-dimensional magnets are vital in this field since they are generally well understood theoretically [3]. In recent years, this enhanced theoretical understanding has been translated into a number of spectacular experimental observations that include a realization of the quantum integrable model with extended E_8 symmetry [4–6], many-body string excitations [7–9], and repulsively bound magnon states [10,11]. Most of these observations are based on spin-1/2 chain materials with pronounced Ising anisotropies, such as $CoNb_2O_6$ [5], $SrCo_2V_2O_8$ [7], and $BaCo_2V_2O_8$ [8]. These materials are more complex than minimalistic theoretical models inspired by them, and important details of their magnetic field B-temperature T phase diagrams remain to be understood [12,13].

Here, we report the experimental discovery of multiple magnetization plateaux in another quasi-one-dimensional magnet with the Ising motif $YbAlO_3$. In contrast with the examples listed above, in $YbAlO_3$ the exchange interaction between spins within the chain is of Heisenberg kind, while that between the spins from neighboring chains is dominantly Ising-like [14,15]. The latter feature originates from the dipole-dipole nature of the interchain interactions [14,16]. It provides a novel route to the incommensurate longitudinal spin-density wave (LSDW) phase, a state that, in many respects, is similar to an itinerant charge-neutral conductor with the magnetic field-dependent Fermi-momenta $k_F = \pi(1 \pm 2M)/2 = \pi(1 \pm m)/2$, where $m = M/M_s$ is the magnetization per site $M = \langle S^z \rangle$ normalized by the saturation value $M_s = 1/2$. We find that LSDW hosts two magnetization plateaux at 1/5 and 1/3 of the saturation value. While the 1/3 plateau has been previously observed in neutron scattering and magnetization studies

*Present address: Department of Applied Physics and Quantum-Phase Electronics Center (QPEC), The University of Tokyo, Bunkyo-ku, Tokyo 113-8656, Japan.
†Contact author: oleg.starykh@utah.edu
‡Contact author: elena.hassinger@tu-dresden.de

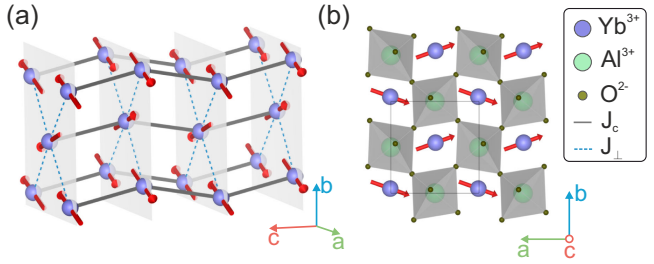

FIG. 1. (a) Sketch of the magnetic structure of $YbAlO_3$ showing only Yb ions and two relevant exchange interactions, J_c and $J_\perp$. (b) Crystal structure of $YbAlO_3$ viewed from the [001] direction.

[16,17], the plateau at $1/5$ is the new result. Notably, both plateaux reported here are detected via the thermal transport and magnetostriction measurements. The measurements are done at sub-Kelvin temperatures ~0.1 K. We find that the intrinsic spin thermal conductivity is larger than the phonon contribution. We present field-theoretic and symmetry-based arguments in favor of the magnetization-plateau stabilization by the ferromagnetic interchain interactions. Furthermore, we detect a phase transition of yet unknown origin not far below the quantum phase transition to the field-polarized state. Our Letter provides new information on the magnetic phase diagram of $YbAlO_3$ and motivates further numerical studies of its microscopic spin Hamiltonian.

Formation of LSDW in $YbAlO_3$—$YbAlO_3$ is a rare-earth-based insulator with an orthorhombically distorted perovskite structure as represented in Fig. 1(b) with room-temperature lattice constants $a = 5.126$, $b = 5.331$, and $c = 7.313$ Å (in conventional $Pbnm$ notation) [18]. Because of the crystal electric fields, the Yb $J = 7/2$ multiplet splits into four doublets, with the lowest-energy doublet well separated from the higher crystal electric field levels, leading to an effective $S = 1/2$ system [14]. The Yb moments have a strong uniaxial g-factor anisotropy with a local easy axis oriented within the ab plane with an angle of $\pm 23.5°$ away from the a axis [Fig. 1(a)] [16,19] and the g factors $g_\parallel = 7.6$ (so that the full magnetic moment is $g_\parallel \mu_B/2 = 3.8\mu_B/\mathrm{Yb}$ [20]), much larger than $g_\perp \approx 0.46$ [14,16,19,20]. Thus, the crystallographic a axis is the direction with the highest and equal g factor for both Yb sites in the crystal structure. In our study, the magnetic field B is applied along this a axis.

The spin chains run along the c axis and are well described by the isotropic Heisenberg intrachain exchange coupling $J_c = 2.4$ K [14,16,21]. Recent neutron scattering reveals a gapless spinon continuum at 1 K, and an antiferromagnetic (AFM) state appears at 0.88 K due to interchain interactions with effective $J_\perp \approx -0.2 J_c = -0.5$ K [16,20,22]. The interchain interactions are likely ferromagnetic and of dipolar origin, leading to an A-type order with distorted ferromagnetic arrangement in the planes perpendicular to the c axis. The magnetic structure and dominant exchange coupling parameters are shown in Fig. 1(a). Surprisingly, the phase diagram of $YbAlO_3$ in magnetic field resembles that of the Ising materials $BaCo_2V_2O_8$ and $SrCo_2V_2O_8$ in which, after suppression of the AFM order at B_c, an incommensurate LSDW order is established because the longitudinal spin-spin correlations are strengthened by the Ising character of the exchange interactions [13,23]. Theoretical studies inspired by $YbAlO_3$ suggest that even for isotropic Heisenberg chains, Ising-like interchain interactions can also stabilize the LSDW [16,22,24,25].

Prime evidence for the LSDW in $YbAlO_3$ comes from the comparison of the Bragg peak position with the magnetization showing exactly the expected behavior [16,17]: the propagation wave vector $\mathbf{Q} = (0, 0, Q)$, where $Q = \pi(1 \pm \delta)$, and the incommensurability $\delta = m = 2M$ scales with the magnetization and is aligned along the chain direction corresponding to the c axis of the crystal, whereas the magnetic moments point along the easy axis direction. Note that $Q = \pm 2k_F$ up to the lattice momentum 2π, characteristic of the LSDW state. As observed previously and reproduced here, Figs. 2(a) and 2(b) show the magnetization plateau state for $M_s/3$ for which Q/π locks into the commensurate position $\delta = 1/3$ in Fig. 2(e) [16,17].

Experimental observation of magnetization plateaux—Figure 2 represents the experimental results of different probes versus field up to the field-polarized state. Additional details are provided in Sec. S1 in Supplemental Material [26]. For each probe, the data are taken at the lowest temperature available. Panels (a) and (b) show, respectively, the magnetization normalized to the saturation value M/M_s and its derivative. As expected, the magnetization rises sharply from zero at $B_c = 0.32$ T and reaches the saturation value M_s at ≈1.4 T at this temperature. The plateau at $\frac{1}{3}M_s$ is clearly visible at a magnetic field of 0.7 T. The field of the quantum critical point $B_{QCP} = 1.15$ T was previously derived [14].

The magnetostriction coefficient, defined as $\lambda = (1/L_0)[dL/dB]$, where L_0 is the sample dimension, was measured along the chain direction and is shown in panel (c). Magnetostriction is a thermodynamic bulk probe that is sensitive to magnetoelastic coupling [35,36]. The signal here is similar to the magnetic susceptibility as seen by comparing panels (c) and (b) ($\Delta L/L_0$ is shown in Fig. S2 in [26]). The $1/3$ plateau is visible in λ as a V-shaped anomaly analogous to the signature in the derivative of the magnetization. Being a very sensitive technique, it also resolves a second smaller V-shaped anomaly at 0.5 T. As indicated by a dashed horizontal line in panel (a), this corresponds to the field where the magnetization reaches $\frac{1}{5}M_s$. Knowing the presence of this anomaly, one can also identify a corresponding small V-shaped signature in the derivative of the magnetization, panel (b). To the best of our knowledge, this is the first time a $1/5$ plateau has been observed in a quantum magnet.

Another anomaly in the magnetostriction is detected at $B^* = 0.96$ T. At this field, the magnetostriction coefficient shows a small but clear jump to a higher value, an unambiguous indication of a weak second-order phase transition, where the slope of the magnetization [panel (b)] also strongly increases to roughly double the value, but less sharply.

We now turn to the thermal conductivity κ, which also contains signatures of all the transitions described above, even though all of the anomalies are broader in the field. Plotted in Fig. 2(d) is the thermal conductivity along the chain direction as a function of magnetic field B relative to its value at zero magnetic field, $\Delta\kappa/\kappa_0 = [\kappa(B) - \kappa_0]/\kappa_0$, where $\kappa_0 = \kappa(B = 0)$ at constant low temperature $T = 108$ mK.

In general, thermal conductivity can give important information on the heat carrying excitations in low-dimensional quantum magnets [37]. For a magnetic insulator such as $YbAlO_3$, phonons and magnetic excitations both contribute to the heat transport, so that $\kappa = \kappa_{ph} + \kappa_{mag}$. For each heat carrier, different scattering mechanisms contribute to the scattering rate. Interactions between the two kinds of heat carriers induce correlations between κ_{ph} and κ_{mag} by reducing both contributions relative to the noninteracting limit. In our data, the low-field $[\kappa(B = 0)]$ and the high-field values of the thermal conductivity at the given temperature agree with each other, as Fig. 2(d) shows. This is because magnetic excitations are gapped in both limits. In the low-field limit, $B < B_c$, the system is in the AFM Ising ordered phase, where the gap in the excitation spectrum is estimated as $T_{gap} = 0.3$ meV$/k_B = 3.5$ K see Fig. 3(b) in [16]. In the high-field limit, $B > 1.5$ T, the spin gap is controlled by the magnetic field. It thus follows that for $T \ll T_{gap}$ there are no magnetic excitations in these magnetic field regions and $\kappa(B = 0)$ represents the upper limit of the phonon contribution to the thermal conductivity. The phonon mean free path is estimated to roughly 100 μm. Conversely, the field-induced increase of $\kappa(B)$ in the intermediate field region $B_c < B < B_{QCP}$ represents the *magnetic* contribution. Moreover, given the detrimental role of the phonon-magnon scattering, $\Delta\kappa$ introduced above represents a *lower* bound of the magnetic thermal conductivity $\kappa_{mag} \geq \Delta\kappa$. (A more detailed discussion of thermal conductivity is presented in the forthcoming publications [38,39].)

This observation explains the high sensitivity of $\Delta\kappa$ in Fig. 2(d) to the magnetic field. As we argue below, the reduction of $\Delta\kappa$ inside the 1/5 and 1/3 plateau phases relative to the increasing κ for the adjacent field regions has to do with the opening of the spin gap inside these *commensurate* SDW states. Such a gap leads to a decrease of the magnetic heat-carrier density and, as a result, a dip in the magnetic thermal conductivity.

Our high-quality data allow for quantitative analysis of the temperature dependence of the anomalies in the plateau states in Figs. 3(a)–3(d). Based on the precise magnetostriction data, we define the width of the plateaux similar as in Ref. [40] (see Fig. 3). For both plateau states, the width remains constant with temperature. The width of the 1/5 plateau is (26 ± 3) mT and roughly 0.4× the width of the 1/3 plateau with (60 ± 5) mT. The anomalies in the curves are visible up to T_N (see a more detailed evaluation of the

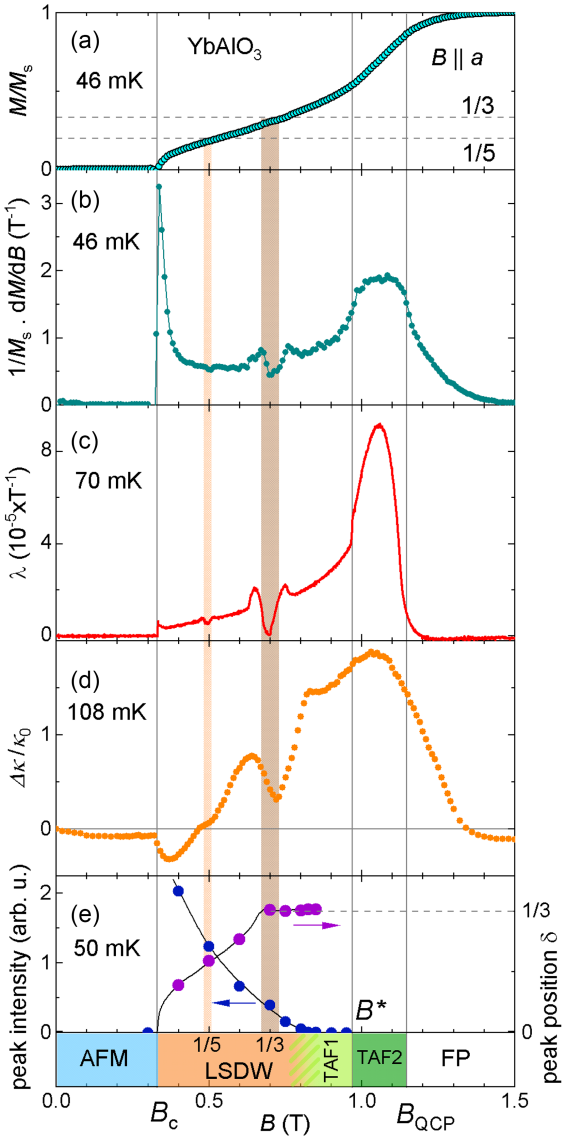

FIG. 2. Field dependence of different quantities in $YbAlO_3$ at low temperature for $H \| a$. Sharp anomalies occur at B_c, B^*, and at the fields where the magnetization reaches $1/5\ M_s$ as well as $1/3\ M_s$ in all quantities: normalized magnetization M/M_s (a), and its derivative (b), magnetostriction coefficient λ (c), and thermal conductivity κ along the chains, here shown as the conductivity change normalized by the zero-field value (d). The 1/3 plateau is also evidenced by a constant position $\mathbf{Q} = (0, 0, Q)$ with $Q = \pi(1 + \delta)$ and $\delta = 1/3$ of the magnetic Bragg peak in neutron scattering [(e), right axis] associated with the LSDW. The Bragg peak intensity is finite and the LSDW state persists up to 0.85 T but becomes very small for fields above 0.75 T [(e), left axis].

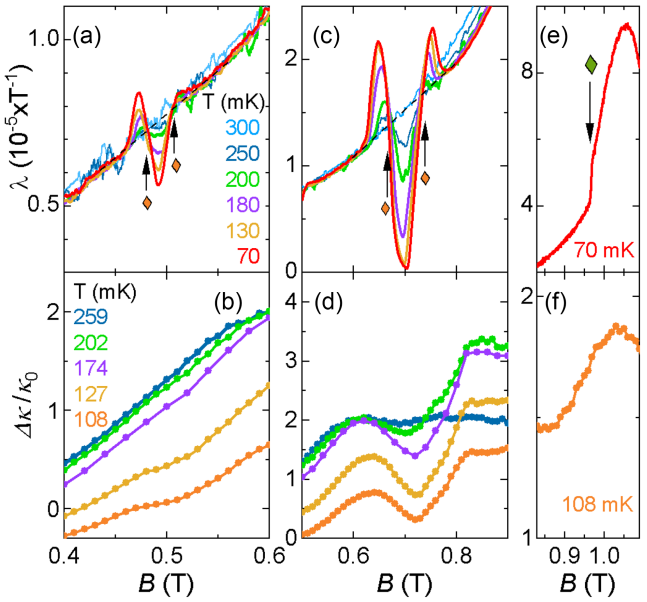

FIG. 3. T evolution of anomalies in magnetostriction and thermal conductivity enlarged around the $1/5$ (a), (b) and $1/3$ (c), (d) plateaux. The plateau region was defined as the field region in which the magnetostriction lies below the high-temperature curve as indicated by the arrows and orange symbols for the curve at 70 mK. (e),(f) An enlargement at the phase transition at $B^* = 0.96$ T at lowest measured temperature, indicated by an arrow and a green symbol in (e).

latter in Sec. S2 in Supplemental Material [26]). From the thermal conductivity we can estimate the size of the gap in the $1/3$ plateau state as given in Sec. S3 in [26], where $\Delta_{1/3}/k_B \approx 0.19$ K.

Theoretical analysis of the plateau states—We now summarize key points of the theoretical analysis of plateau phases which is presented in Sec. S4 in Supplemental Material [26]. Magnetization plateau states represent a *commensurate* version of the LSDW phase. Once the latter is stabilized by the magnetic field and interchain spin interactions, the plateaux are bound to happen as the LSDW ordering wave vector $q = 2k_F$ continuously scans the interval from π at $M = 0$ to 0 at $M = 1/2$. In the process, it passes through fractional values ν/k (ν and k are *integers*) of the reciprocal lattice vector 2π. For each of these occurrences, there exists a symmetry-allowed *umklapp* interaction that involves k spins and changes the total momentum of the spin subsystem by $2\pi\nu$, i.e., by ν units of the lattice momentum. For a single Heisenberg spin chain, such multiparticle interactions are highly irrelevant and do not affect the magnetization [3]. However, in the *ordered* three-dimensional LSDW phase, they do produce plateaux at magnetization $M_{\nu,k} = (1 - 2\nu/k)/2$ *provided* that the corresponding k th order umklapp interaction also minimizes the much stronger interchain interaction (which is the reason for the LSDW phase in the first place). Finally, the width of the plateau (in the magnetic field) is exponentially narrow in k^2, which strongly favors plateaux with the smallest possible k values. The detailed phenomenological analysis in Sec. S4 in [26] shows that ferromagnetic interchain interaction favors *odd-k* umklapps. Together with the experimental restriction that the LSDW phase occupies a finite magnetization interval $0 < 2M \leq 1/3$ (see the section on the phase diagram below), one concludes that plateaux at $M_{1,3}$ and $M_{2,5}$ are the most prominent ones satisfying all the requirements. Moreover, the $M_{2,5}$ plateau is narrower than the $M_{1,3}$ one, precisely as the experiment shows. Theoretically, the next most stable plateau in the available magnetization range is $M_{3,7}$, at $1/7$ of M_s. The arguments above, together with the fact that $7^2/5^2 \approx 2$, predict that it should be much narrower than the already tiny $M_{2,5}$ feature, explaining its absence in our data.

It is worth noting here that the AFM phase itself, in fact, is a *zero* magnetization plateau, $M_{1,2}$ in our notations. Unlike all other plateaux discussed above, it is an *even-k* ($k = 2$) state. Correspondingly, it will be present even if the interchain interaction is antiferromagnetic. Being the smallest-k plateau, it is, in agreement with the theory, the widest one in the magnetic field. The AFM-LSDW transition is, therefore, of the commensurate-incommensurate (C-IC) kind. A sharp variation of the ordering wave vector Q with B in Fig. 2(e), where Q deviates from its commensurate π value with an infinite slope, is a clear experimental manifestation of the C-IC physics [26].

The phase diagram—Our findings, together with the previously available data, are summarized in the phase diagram in Fig. 4. The phase diagram is guided by theoretical studies [16,22,24,25] which suggest the following sequence of the phases: Ising AFM-LSDW-TAF-FP. Here, the transverse antiferromagnetic phase (TAF) denotes

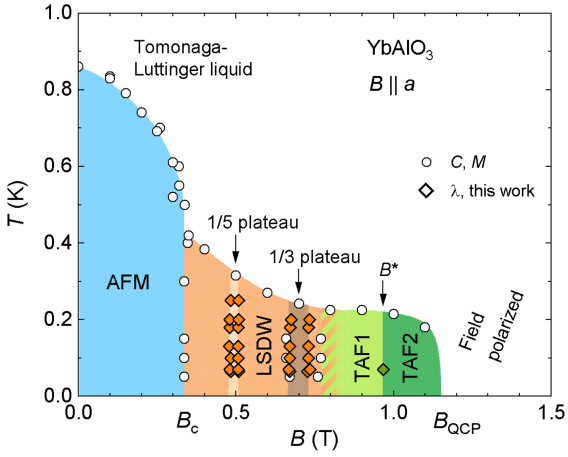

FIG. 4. The phase diagram of $YbAlO_3$. White points are from specific heat C and magnetization M in Ref. [16]. Orange and green points are from the magnetostriction λ in this work showing the two plateau regions appearing within the LSDW state and the phase transition at $B^* = 0.96$ T. See text for details.

a commensurate state with $Q = \pi$ and staggered spin order in the plane perpendicular to the easy axis. Neutron scattering detection of this high-field phase is severely complicated by the high anisotropy of the g factor in $YbAlO_3$. Compared to the longitudinal signal, any transverse signal is reduced by a factor $(g_\parallel/g_\perp)^2 \approx 273$. FP denotes the field-polarized ferromagnetic phase.

Based on the data, LSDW phase extends from B_c to about 0.75 T corresponding roughly to the upper end of the $1/3$ plateau given that the upper end varies with measurement technique and definition. While the LSDW Bragg peak in Fig. 2(e) persists beyond this field, its intensity drops strongly for $B > 0.75$ T. Given the different symmetries of the LSDW and TAF phases and their respective ordering wave vectors Q, the transition between them is likely of the first order. This explains the persistence of the LSDW Bragg peak into a coexistence region between 0.75 and 0.85 T. The change from LSDW to TAF is also seen in the flattening of the critical temperature T_N curve in Fig. 4. Figure S5 shows the elastic Bragg signal from the TAF phase in the interval from 0.75 T to the saturation. We note that this analysis is slightly complicated by the presence of the small twin crystallite in the studied sample, as is discussed in detail in Sec. S5 in Supplemental Material [26]. It also must be noted that the very existence of the TAF phase requires some interaction between *transverse* (with respect to the field) components of spins on neighboring chains [22]. Comparing the ratio of the widths of TAF and LSDW phases with that in the theoretical phase diagram in [22], we can estimate the degree of the interchain exchange anisotropy as $\epsilon = J_\perp^{xy}/J_\perp^z \approx 0.15$. The small value of this estimate supports our assumption of the dominant Ising-like nature of the interchain interaction.

The transition at B^*, evidenced in Fig. 2(c), and the exact nature of the phases remain not understood. We label them as TAF1 and TAF2 because the ordering vector detected in neutron scattering stays the same, see Fig. S5. One possibility is a change in the transverse moment orientation at this field, since $g_\perp$ along the c and b axes might be different. The situation could also be similar to $BaCo_2V_2O_8$ which too features an unknown high-field state between the TAF and FP ones [12,13]. We speculate that such an additional phase may be caused by the dipole-dipole interaction between spin chains.

Summary—Magnetization plateaux in spin-1/2 quantum magnets are rare and interesting. Their previous sightings include the $M_s/3$ plateau state, also known as the *up-up-down* state, in spatially anisotropic triangular antiferromagnets Cs_2CuBr_4 [41] and Cs_2CoBr_4 [42]. As explained above, magnetization plateaux are to be expected in quasi-one-dimensional magnets supporting the field-induced LSDW phase. Yet, Ising-like chain materials $BaCo_2V_2O_8$ and $SrCo_2V_2O_8$ that do feature the LSDW phase do not appear to contain any finite-M plateaux. We attribute this difference with $YbAlO_3$ to the *antiferromagnetic* sign of the interchain interaction, which suppresses the *odd-k* plateaux, in those Co-based magnets.

To the best of our knowledge, the reported observation of the *two* plateaux, at magnetizations $M_{2,5}$ and $M_{1,3}$, is the first of its kind. The fact that this is done with the help of heat transport measurement makes it even more rare. We hope that our findings generate further interest in the unusual ordered states of quasi-one-dimensional magnetic materials.

Note added—Recently, our new magnetic susceptibility measurement revealed evidence for a plausible 1/7 magnetization plateau as a small but persistent feature (see Fig. S3 in Supplemental Material [26]). This finding further supports the theoretical interpretation of the data presented here.

Acknowledgments—We thank Cristian Batista, Leon Balents, Achim Rosch, Rong Yu, Jianda Wu, Burkhard Schmidt, Andy Mackenzie, and the participants of the KITP QMagnets23 program for fruitful discussions. E. H. acknowledges funding from Deutsche Forschungsgemeinschaft (DFG) for the projects CRC 1143–Project No. 247310070 (project C10) and the Wuerzburg-Dresden cluster of excellence EXC 2147 "ct.qmat Complexity and Topology in Quantum Matter"–Project No. 390858490. Furthermore, E. H. and P. M. acknowledge support from the DFG for the CRC 80–Project No. 107745057 (project E03) and from the Max Planck Society for the research group "Physics of Unconventional Metals and Superconductors" and the Max-Planck Fellowship. O. A. S. acknowledges support by the NSF CMMT Grant No. DMR-1928919. This research was supported in part by Grant No. NSF PHY-2309135 to the Kavli Institute for Theoretical Physics (KITP).

Data availability—The data that support the findings of this Letter are not publicly available. The data are available from the authors upon reasonable request.

[1] L. Savary and L. Balents, Rep. Prog. Phys. **80**, 016502 (2016).
[2] O. A. Starykh, Rep. Prog. Phys. **78**, 052502 (2015).
[3] T. Giamarchi, *Quantum Physics in One Simension*, The International Series of Monographs on Physics (Clarendon, Oxford, 2003).
[4] A. B. Zamolodchikov, Int. J. Mod. Phys. A **04**, 4235 (1989).
[5] R. Coldea, D. A. Tennant, E. M. Wheeler, E. Wawrzynska, D. Prabhakaran, M. Telling, K. Habicht, P. Smeibidl, and K. Kiefer, Science **327**, 177 (2010).
[6] J. Wu, M. Kormos, and Q. Si, Phys. Rev. Lett. **113**, 247201 (2014).
[7] Z. Wang, J. Wu, W. Yang, A. K. Bera, D. Kamenskyi, A. T. M. N. Islam, S. Xu, J. M. Law, B. Lake, C. Wu, and A. Loidl, Nature (London) **554**, 219 (2018).

[8] Z. Wang, M. Schmidt, A. Loidl, J. Wu, H. Zou, W. Yang, C. Dong, Y. Kohama, K. Kindo, D. I. Gorbunov, S. Niesen, O. Breunig, J. Engelmayer, and T. Lorenz, Phys. Rev. Lett. **123**, 067202 (2019).
[9] J. Yang, T. Xie, S. E. Nikitin, J. Wu, and A. Podlesnyak, Phys. Rev. B **108**, L020402 (2023).
[10] C.-M. Halati, Z. Wang, T. Lorenz, C. Kollath, and J.-S. Bernier, Phys. Rev. B **108**, 224429 (2023).
[11] Z. Wang, C.-M. Halati, J.-S. Bernier, A. Ponomaryov, D. I. Gorbunov, S. Niesen, O. Breunig, J. M. Klopf, S. Zvyagin, T. Lorenz, A. Loidl, and C. Kollath, Nature (London) **631**, 760 (2024).
[12] M. Klanjšek, M. Horvatić, S. Krämer, S. Mukhopadhyay, H. Mayaffre, C. Berthier, E. Canévet, B. Grenier, P. Lejay, and E. Orignac, Phys. Rev. B **92**, 060408(R) (2015).
[13] S. Takayoshi, Q. Faure, V. Simonet, B. Grenier, S. Petit, J. Ollivier, P. Lejay, and T. Giamarchi, Phys. Rev. Res. **5**, 023205 (2023).
[14] L. S. Wu, S. E. Nikitin, M. Brando, L. Vasylechko, G. Ehlers, M. Frontzek, A. T. Savici, G. Sala, A. D. Christianson, M. D. Lumsden, and A. Podlesnyak, Phys. Rev. B **99**, 195117 (2019).
[15] L. S. Wu, W. J. Gannon, I. A. Zaliznyak, A. M. Tsvelik, M. Brockmann, J.-S. Caux, M. S. Kim, Y. Qiu, J. R. D. Copley, G. Ehlers, A. Podlesnyak, and M. C. Aronson, Science **352**, 1206 (2016).
[16] L. S. Wu, S. E. Nikitin, Z. Wang, W. Zhu, C. D. Batista, A. M. Tsvelik, A. M. Samarakoon, D. A. Tennant, M. Brando, L. Vasylechko, M. Frontzek, A. T. Savici, G. Sala, G. Ehlers, A. D. Christianson, M. D. Lumsden, and A. Podlesnyak, Nat. Commun. **10**, 698 (2019).
[17] S. E. Nikitin, S. Nishimoto, Y. Fan, J. Wu, L. S. Wu, A. S. Sukhanov, M. Brando, N. S. Pavlovskii, J. Xu, L. Vasylechko, R. Yu, and A. Podlesnyak, Nat. Commun. **12**, 3599 (2021).
[18] O. Buryy, Y. Zhydachevskii, L. Vasylechko, D. Sugak, N. Martynyuk, S. Ubizskii, and K. D. Becker, J. Phys. Condens. Matter **22**, 055902 (2010).
[19] D. Ehlers, L. Vasylechko, Z. Medvecka, and J. Sichelschmidt, Appl. Magn. Reson. **53**, 1399 (2022).
[20] P. Radhakrishna, J. Hammann, M. Ocio, P. Pari, and Y. Allain, Solid State Commun. **37**, 813 (1981).
[21] S. E. Nikitin, T. Xie, A. Podlesnyak, and I. A. Zaliznyak, Phys. Rev. B **101**, 245150 (2020).
[22] Y. Fan and R. Yu, Chin. Phys. B **29**, 057505 (2020).
[23] K. Okunishi and T. Suzuki, Phys. Rev. B **76**, 224411 (2007).
[24] Y. Fan, J. Yang, W. Yu, J. Wu, and R. Yu, Phys. Rev. Res. **2**, 013345 (2020).
[25] C. E. Agrapidis, J. van den Brink, and S. Nishimoto, Phys. Rev. B **99**, 224423 (2019).
[26] See Supplemental Material at http://link.aps.org/supplemental/10.1103/grfl-37g2 which contains descriptions of the experimental methods and protocols, data of the magnetic susceptibility showing the 1/7 plateau, some further analysis, and details about the theory. Supplemental Material also includes Refs. [27–34].
[27] M. A. Noginov, G. B. Loutts, K. Ross, T. Grandy, N. Noginova, B. D. Lucas, and T. Mapp, J. Opt. Soc. Am. B **18**, 931 (2001).
[28] T. Sakakibara, H. Mitamura, T. Tayama, and H. Amitsuka, Jpn. J. Appl. Phys. **33**, 5067 (1994).
[29] R. Küchler, R. Wawrzyńczak, H. Dawczak-Dębicki, J. Gooth, and S. Galeski, Rev. Sci. Instrum. **94**, 045108 (2023).
[30] R. Küchler, A. Wörl, P. Gegenwart, M. Berben, B. Bryant, and S. Wiedmann, Rev. Sci. Instrum. **88**, 083903 (2017).
[31] M. Nikolo, Am. J. Phys. **63**, 57 (1995).
[32] O. A. Starykh, H. Katsura, and L. Balents, Phys. Rev. B **82**, 014421 (2010).
[33] O. A. Starykh and L. Balents, Phys. Rev. B **89**, 104407 (2014).
[34] E. M. Stoudenmire and L. Balents, Phys. Rev. B **77**, 174414 (2008).
[35] V. S. Zapf, V. F. Correa, P. Sengupta, C. D. Batista, M. Tsukamoto, N. Kawashima, P. Egan, C. Pantea, A. Migliori, J. B. Betts, M. Jaime, and A. Paduan-Filho, Phys. Rev. B **77**, 020404(R) (2008).
[36] A. Miyata, T. Hikihara, S. Furukawa, R. K. Kremer, S. Zherlitsyn, and J. Wosnitza, Phys. Rev. B **103**, 014411 (2021).
[37] C. Hess, Phys. Rep. **811**, 1 (2019).
[38] P. Mokhtari, U. Stockert, S. E. Nikitin, L. Vasylechko, M. Brando, and E. Hassinger (unpublished).
[39] P. Mokhtari *et al.* (unpublished).
[40] K. M. Ranjith, S. Luther, T. Reimann, B. Schmidt, P. Schlender, J. Sichelschmidt, H. Yasuoka, A. M. Strydom, Y. Skourski, J. Wosnitza, H. Kühne, T. Doert, and M. Baenitz, Phys. Rev. B **100**, 224417 (2019).
[41] N. A. Fortune, S. T. Hannahs, Y. Yoshida, T. E. Sherline, T. Ono, H. Tanaka, and Y. Takano, Phys. Rev. Lett. **102**, 257201 (2009).
[42] L. Facheris, K. Y. Povarov, S. D. Nabi, D. G. Mazzone, J. Lass, B. Roessli, E. Ressouche, Z. Yan, S. Gvasaliya, and A. Zheludev, Phys. Rev. Lett. **129**, 087201 (2022).